New Journal of Chemistry

Structural Features, Magnetic Properties and Photocatalytic Activity of Bismuth Ferrite Nanoparticles Grafted on Graphene Nanosheets

Om Prakash Bajpai[a], Subrata Mandal[b], Rajakumar Ananthakrishnan[b], Pijush Mandal[a], Dipak Khastgir[a], Santanu Chattopadhyay[a,*]

[a] Rubber Technology Centre, Indian Institute of Tech nology Kharagpur 721302, India

[b] Department of Chemistry, Indian Institute of Technology, Kharagpur 721302, India

*Corresponding author: Santanu Chattopadhyay, E-Mail: santanuchat71@yahoo.com

Tel.: +91-3222 281758, Fax: +913222 282292
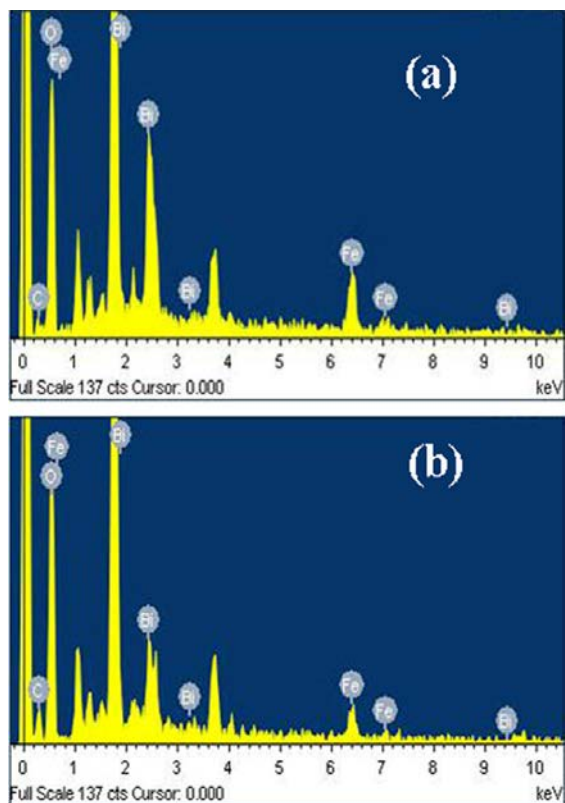
Figure S1. (a, b) the EDX spectra of $BiFeO_3$-*g*-GNS corresponding to the HRTEM images shown in the figure 5c and 5d.

Figure S2 illustrates FTIR spectra of GNS and BiFeO$_3$-g-GNS. The absorption bands at 3428 cm^{-1} (O-H stretching vibrations), 1730 cm^{-1} (C=O stretching vibrations), 1575-1630 cm^{-1} (skeletal vibrations from un-oxidized graphite), 1438 cm^{-1} (C-OH stretching vibrations), 1092 cm^{-1} (C-O stretching vibrations) and 1260 cm^{-1} (C-O-C stretching vibrations), are present in both GNS and BiFeO$_3$-g-GNS. However in case of BiFeO$_3$-g-GNS, slight shifting of these peaks (toward lower wavenumber) can be observed in Figure S2. Thus, FTIR spectra also indicate the enhanced chemical interaction between BiFeO$_3$ and GNS. Also, the peaks at 2924 cm^{-1} and 2853 cm^{-1} are characteristics of asymmetric and symmetric -CH$_2$ stretching vibrations. The FTIR results also match with the reported literature[1]. Refer to our previous publication for the FTIR spectra of pristine BiFeO$_3$ [2].
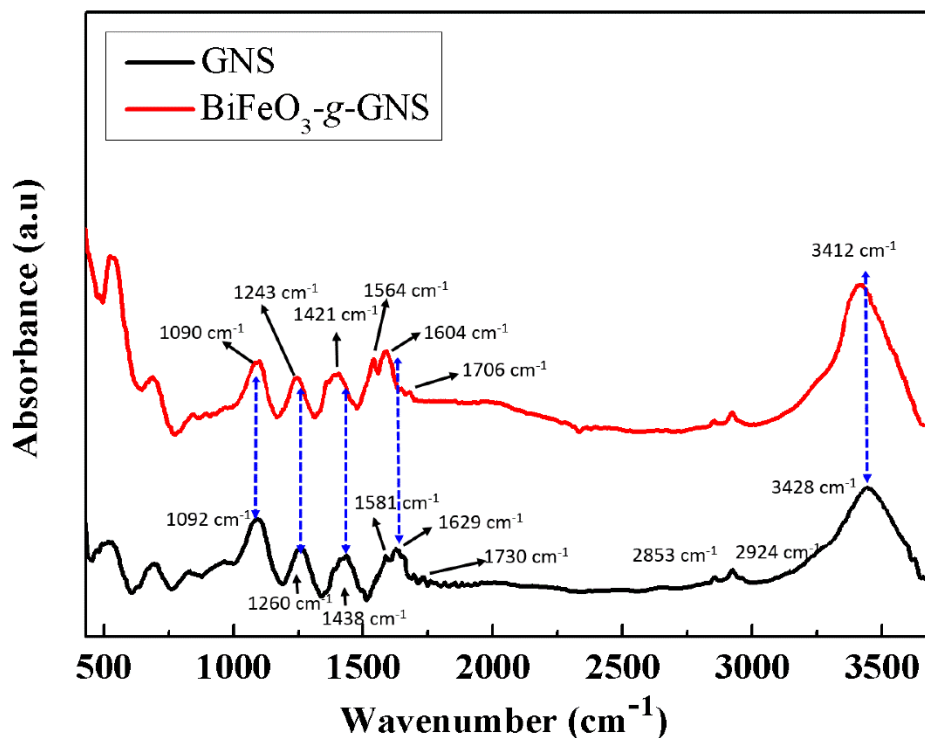
Figure S2. FTIR spectra of pristine GNS and BiFeO$_3$-g-GNS.

Optical characteristics of the photocatalyst were further investigated by photoluminescence (PL) spectroscopy. It is well established fact that electron-hole recombination directly depends on PL

intensity of the material [3-4]. Low PL intensity indicates the inhibition of recombination between electrons and holes. Figure S3 shows that in case of $BiFeO_3$-g-GNS, PL intensity decreases significantly than pristine $BiFeO_3$. Hence, the rate of recombination of electron and hole is diminished in $BiFeO_3$-g-GNS.
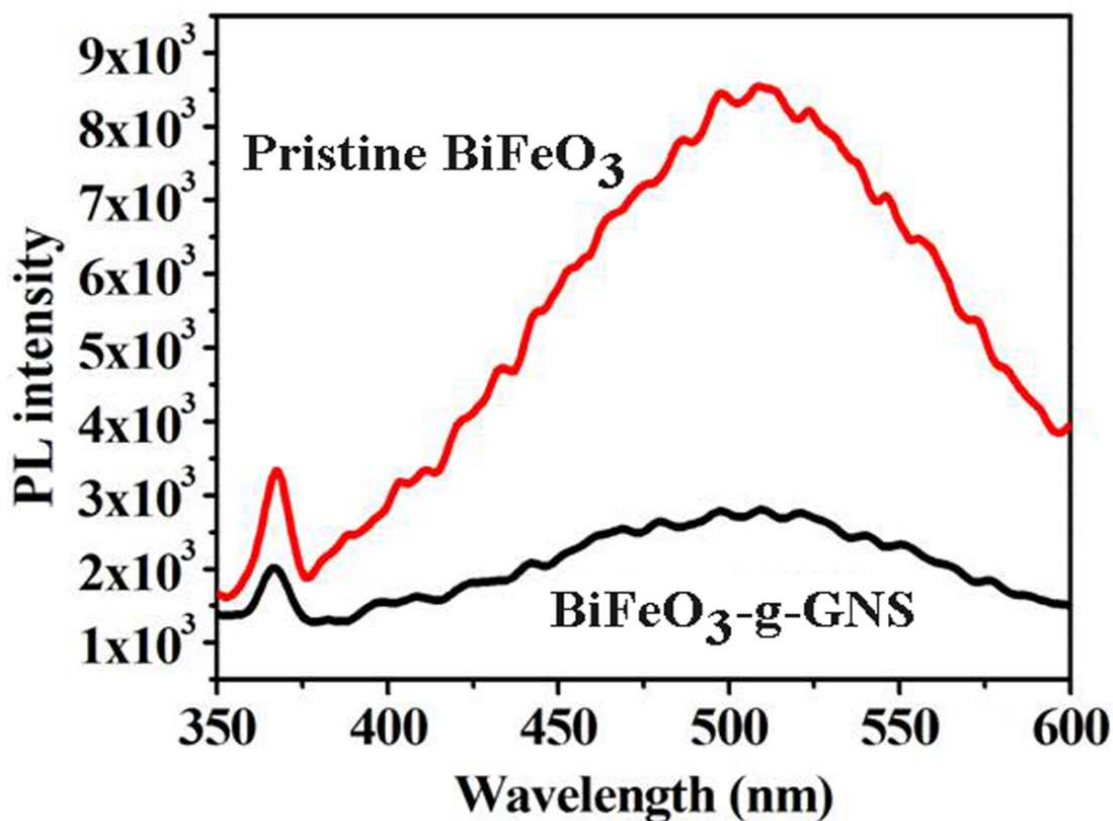
Figure S3. PL curves of pristine $BiFeO_3$ and $BiFeO_3$-g-GNS.

Here, Figure S4 shows N_2 (77 K) adsorption–desorption characteristics of pristine $BiFeO_3$ and $BiFeO_3$-g-GNS. Total specific surface area of the photocatalyst was obtained through Brunauer-Emmett-Teller (BET) calculations. It has been observed that surface area increases significantly in case of $BiFeO_3$-g-GNS (70.56 m^2/g) than pristine $BiFeO_3$ (44.01 m^2/g). Also, slight reduction of pore size was observed. Hence, it is expected that photocatalytic activity of $BiFeO_3$ might be enhanced by due to increased surface area by the incorporation of GNS.
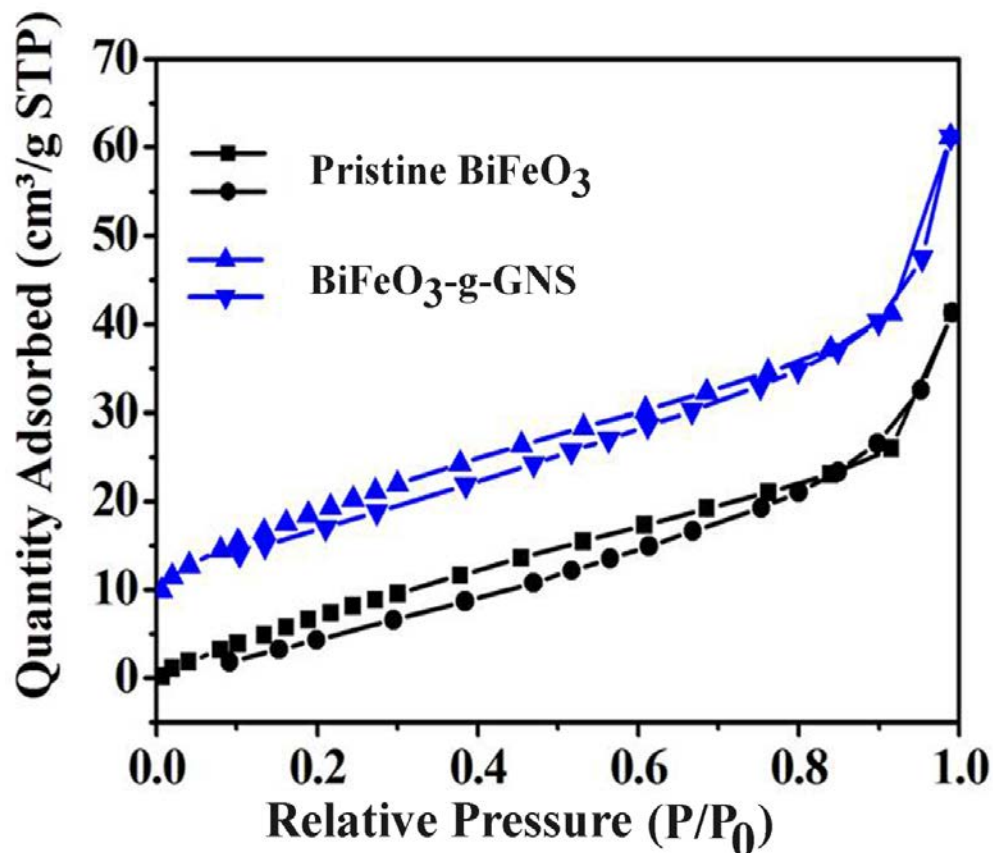
Figure S4. Nitrogen (77 K) adsorption–desorption isotherms of pristine $BiFeO_3$ and $BiFeO_3$-*g*-GNS.

Table S1: BET surface area, pore volume and pore size of pristine $BiFeO_3$ and $BiFeO_3$-*g*-GNS.

Catalysts	Surface Area (m²/g)	Pore Volume (cm³/g)	Pore Size (Å)
Pristine $BiFeO_3$	44.018	0.0600	65.416
$BiFeO_3$-*g*-GNS	70.569	0.0904	58.693

To confirm the light sensitivity and active role of photocatalyst in the degradation of dyes, we have performed dark adsorption assay with $BiFeO_3$-*g*-GNS for 60 min. Figure S5 & S6 show

that only 9.5% and 6.1% degradation were observed for MB and MO respectively in dark (60 min) (Table S2). This confirms that significant degradation of both dyes take place only under light irradiation. Moreover, the observation also proves that degradation of dye mainly occurs due the active role of photocatalyst and not because of the surface adsorption.
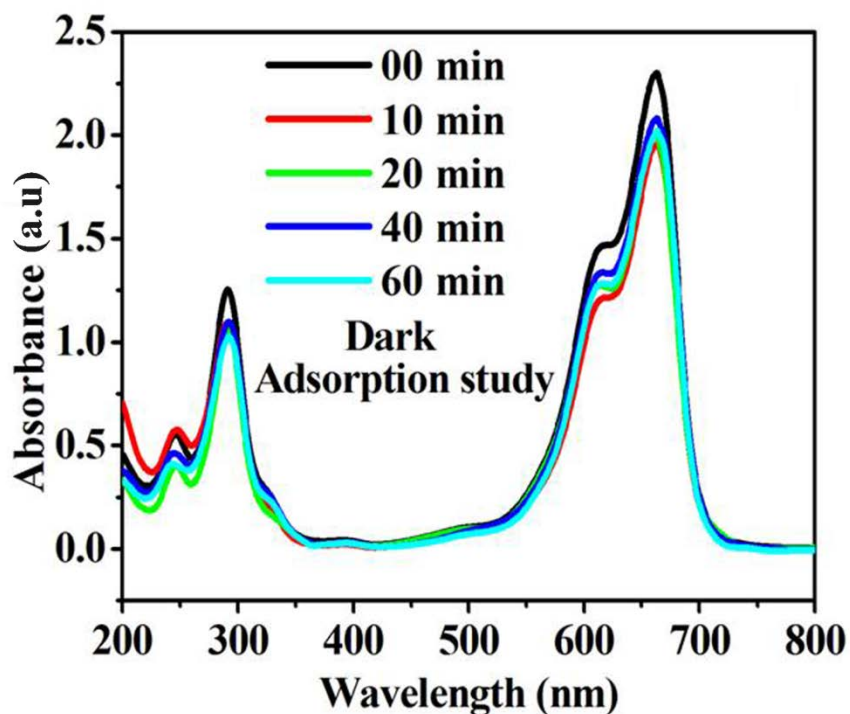
Figure S5. UV-visible absorption spectra of MB in presence of $BiFeO_3$-g-GNS in dark at regular time interval.
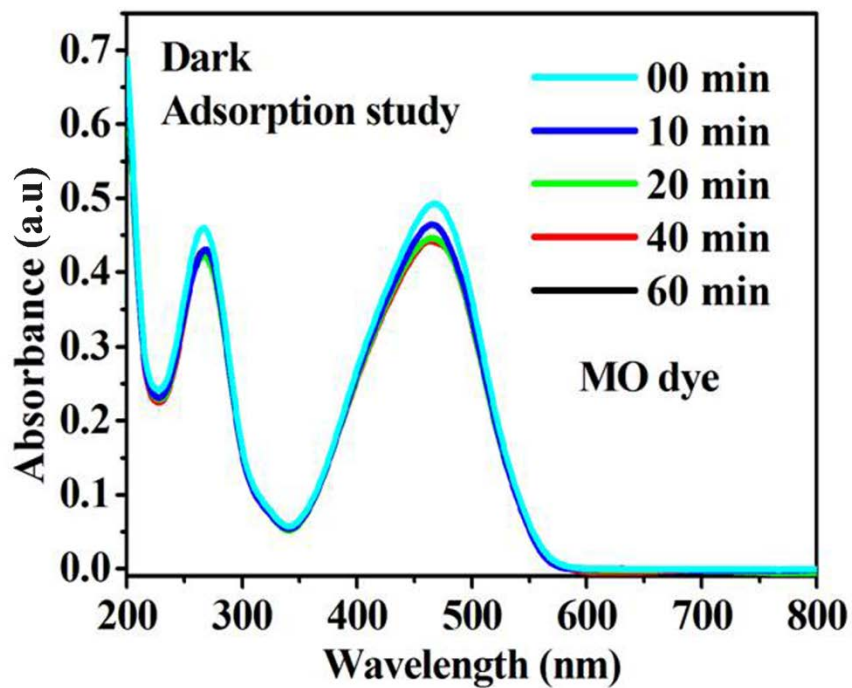
Figure S6. UV-visible absorption spectra of MO in presence of BiFeO$_3$-g-GNS in dark at regular time interval.

Table S2: Dark adsorption assay details of dyes in presence of BiFeO$_3$-g-GNS photocatalyst

Name of dye	Catalytic dose (mg/ml)	MB dye (mgL^{-1})	Time in dark condition (min)	% of degradation
MB	1	20	60	9.5
MO	1	20	60	6.1

Kubelka-Munk model has been used for determining the band gap of the samples. The model depends on the interaction of incoming light with the fine layer of material. Here, illuminated light must be diffused and monochromatic. Moreover, material should be uniform, isotropic, non-fluorescent and non-glassy. Kubelka-Munk calculated reflectance from the layer which is capable of scattering and absorbing the light. They have derived an equation for optical absorption coefficient α and band gap:

$$\alpha h v = \sqrt[n]{A(h v - Eg)}$$

where h is the Plank constant and ν represents frequency of light, Eg − band gap, and A-absorption constant.

This is called Kubelka-Munk equation. From the equation, the optical band gap of the samples can be obtained from the plots of $(\alpha h v)^2$ *vs.* photon energy $(h v)$ by extrapolating the straight line to the axis intercept (figure 10 of main manuscript). Overall percentage degradation of MB and MO dyes in the presence of $BiFeO_3$-*g*-GNS with 60 min of irradiation was more (87% and 35.9%, respectively) than in the presence of pristine $BiFeO_3$ (57.9 and 4.1%, respectively) photocatalyst. Thus, it is apparent that $BiFeO_3$-*g*-GNS show rapid degradation of both the dyes under the visible light condition.

 The efficiency of photo-degradation can be calculated by the following equation:

$$\eta(\% \, degradation) = [\frac{C_0 - C_t}{C_0}] \times 100$$

Where C_0 represents initial concentration of dye (t=0) and C_t is concentration of dye at t= t (at different time interval)

Table S3: Rate constants and percentage degradation of MB dye in the (i) absence of photocatalyst, (ii) pristine $BiFeO_3$ and (iii) $BiFeO_3$-g-GNS.

Photocatalyst	Catalytic dose (mg/ml)	MB dye (mgL^{-1})	Irradiation time (min)	Rate constant (min^{-1})	% of degradation
-	1	20	60	1.4×10^{-3}	9.8
Pristine $BiFeO_3$	1	20	60	10.2×10^{-3}	57.9
$BiFeO_3$-g-GNS	1	20	60	22.4×10^{-3}	87

Table S4: Photocatalytic rate constant and percentage degradation of MO dye in the (i) absence of photocatalyst, (ii) pristine $BiFeO_3$ and (iii) $BiFeO_3$-g-GNS.

Photocatalyst	Catalytic dose (mg/ml)	MO dye (mgL^{-1})	Irradiation time (min)	Rate constant (min^{-1})	% of degradation
-	-	20	60	0.13×10^{-3}	2.2
Pristine $BiFeO_3$	1	20	60	0.30×10^{-3}	4.1
$BiFeO_3$-g-GNS	1	20	60	2.62×10^{-3}	35.9
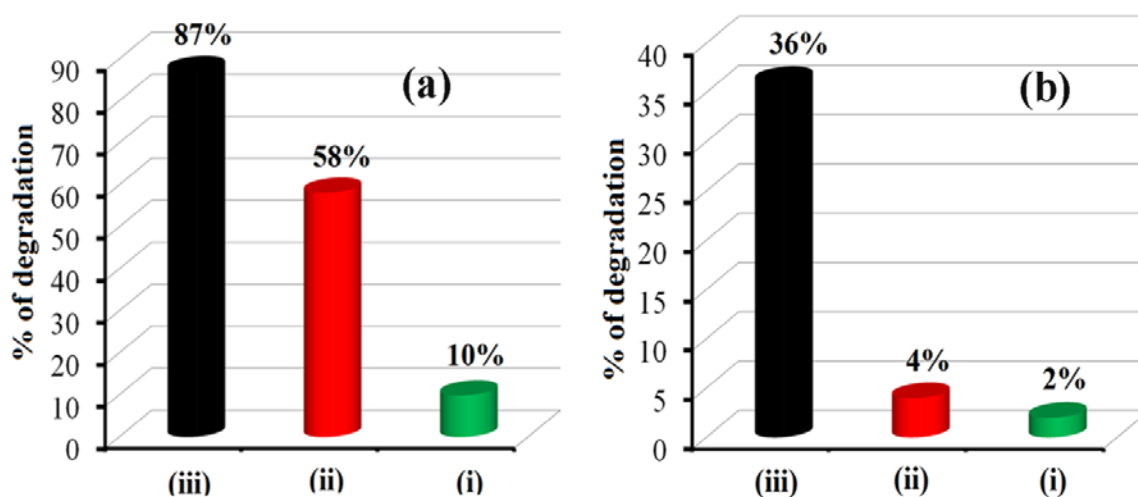
Figure S7. Photocatalytic degradation percentages of (a) MB, and (b) MO dyes at the end of 60 min in the (i) absence of photocatalyst, (ii) pristine $BiFeO_3$ and (iii) $BiFeO_3$-g-GNS.
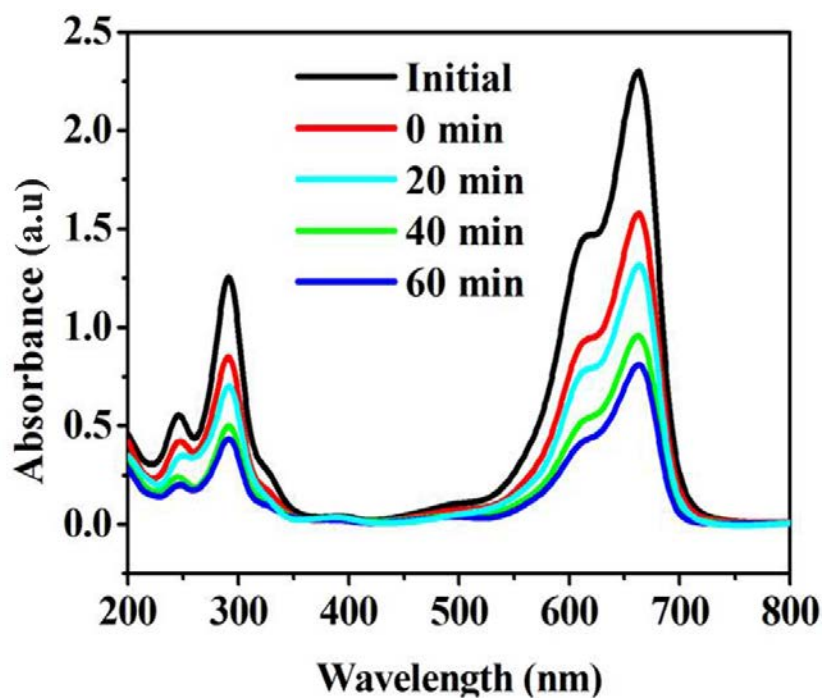
Figure S8. UV-visible absorption spectra of MB in the presence of $BiFeO_3$-*g*-GNS containing 20 wt% $BiFeO_3$ under light at regular time interval.
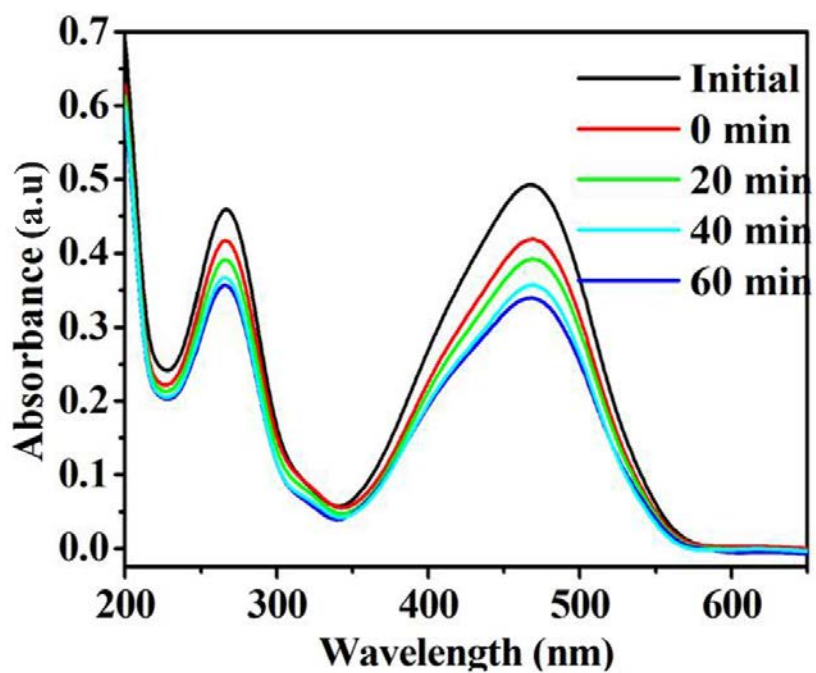
Figure S9. UV-visible absorption spectra of MO in the presence of $BiFeO_3$-*g*-GNS containing 20 wt% $BiFeO_3$ under light at regular time interval.

Table S5: MB and MO dyes degradation in the presence of BiFeO$_3$-g-GNS containing 20 wt% BiFeO$_3$

Name of dye	Catalytic dose (mg/ml)	MB dye (mgL^{-1})	Irradiation time (min)	% of degradation
MB	1	20	60	65.4
MO	1	20	60	30.1

References

1. Hu, Zhong-Ting, *et al., Chem. Eng. J.* **2015**, 262, 1022-1032.

2. Bajpai, O. P. *et al. Express Polym. Lett.* **2014**, 8, 669-681.

3. Md. Rakibuddin; Ananthakrishnan, R., *New J. Chem.* **2016,** *40*, 3385-3394.

4. Li, Y.; *et al., Langmuir* **2008,** *24*, 8351-8357.